ABSTRACT

Title of Thesis: INTERCALATED MoS_2 NANOPARTICLES FOR ENHANCED

DISPERSION IN SMOKES AND OBSCURANTS

D'Anne Emmett Spence, Master of Science, 2003

Thesis Directed by: Professor Bryan W. Eichhorn
                      Department of Chemistry and Biochemistry

The intercalation of MoS_2 with diethyl oxalate (DEO) and Meldrum's Acid (MA) has been achieved via an exfoliation and reflocculation process. Ethyl diazoacetate (EDA) did not intercalate under identical conditions. The resulting compounds, $Li_{0.1}MoS_2(DEO)_{0.10}$ and $Li_{0.1}MoS_2(MA)_{0.14}$, have the metastable 1T-MoS_2 crystal structure and have been characterized by XRD, TGA, NMR, and DSC. Based on XRD analysis, the intercalated compounds are trigonal with P3 crystal symmetry where $a = b = 3.36$ Å and c, which varies with the intercalate, is 10.20 Å and 9.97 Å for $Li_{0.1}MoS_2(DEO)_{0.10}$ and $Li_{0.1}MoS_2(MA)_{0.14}$, respectively. The concentration of the DEO and MA in the intercalated compounds, 0.10 and 0.14, respectively, was calculated using air TGA data and supported by nitrogen TGA data and NMR. The structural models of the new compounds are described within.

INTERCALATED MoS$_2$ NANOPARTICLES FOR ENHANCED DISPERSION IN

SMOKES AND OBSCURANTS

by

D'Anne Emmett Spence

Thesis submitted to the Faculty of the Graduate School of the
University of Maryland, College Park in partial fulfillment
of the requirements for the degree of
Master of Science
2003

Advisory Committee:

    Professor Bryan W. Eichhorn, Chair
    Professor Lawrence R. Sita
    Professor Andrei N. Vedernikov
    Professor Robert Walker

DEDICATION

To my parents, whose love, support, and example have helped me find my dreams and to

Chad for never letting me give up.

ACKNOWLEDGMENTS

I think if any of us honestly reflects on who we are, how we got here, what we think we might do well, we discover a debt to others that spans written history. The work of some unknown person makes our lives easier everyday. I believe it's appropriate to acknowledge all of these unknown persons; but it is also necessary to acknowledge those people we know have directly shaped our lives and our work. This page is specifically designed to note my appreciation to those people who stand out most notably in my mind as contributing to the content of what you will find in this thesis.

First and foremost I would like to thank my advisor, Dr. Bryan Eichhorn, for understanding my compressed schedule and additional military duties. It is doubtful I would have learned and accomplished as much as I did in a year and a half without his support and for that I am truly grateful. I also appreciate all of his great restaurant recommendations.

I would also like to thank Jim Watson to whom I am eternally indebted. His amazing gift as a teacher has helped me to "say what I mean" by letting me pick his brain for the "right" chemistry words. In the short time I have known him, he has taught me a lot about science, a little about life, and how to have packages mailed to the chemistry department. For all of those things I am truly thankful. I have lost track of all of the favors I owe him and as I prepare to leave I know I will continue to call on him in both personal and professional matters.

Immeasurable thanks also go to Emily Weinert and Amy Finch. Without them I would have never made it through this program. I cherish their friendship and appreciate

their ability to always make me laugh when I am having a bad day. I will miss the late night study sessions, girls' night out, cumulative exam nights, and Los Ponchos lunches, however; it is their friendship that I will miss the most when I leave.

Melanie Moses and Chad Stoltz also deserve special mention. My NMR data would not have been possible without Melanie's help. She agreed to run two samples and even though it ended up being 20 she was always accommodating to my needs. Melanie has also become a good friend who helped me realize that I could write this thesis. Thanks for all of the editing! Chad helped me understand solid state chemistry and kept the XRD up and running, without both I could have never completed my project. Other graduate students in my lab I would like to thank are Emren Esenturk and Oktay Demircan. Their smiles and encouragement throughout the year helped me more then they will ever know. I appreciate the time they took to answer my questions and help me become a better critical thinker. Hopefully they will be my Turkish tour guides one day soon.

Jen Gresham, my Air Force mentor, who I think was shocked when I became an inorganic chemist always seemed to know when I needed a lunch break thanks. I cannot believe that we live less than five minutes from each other and never made it to dinner in Bethesda together. We are lame! Her hard work inspired me and I look forward to working with her in Colorado Springs.

Last, but certainly not least, to my husband Chad for understanding all of the late nights, the long weekends, and how important this degree is to me. I could not have done this without you.

TABLE OF CONTENTS

LIST OF TABLES

LIST OF FIGURES

Introduction

There has been an increased interest in the use of smokes and obscurants to protect various military ground assets. As lethality targeting improves, new concealment technologies must be created to allow real time asset protection in the field. Smokes and obscurants are a facet of concealment technologies, which are actively deployed in the air to screen assets from enemy detection. Ideal smokes and obscurants should be able to effectively block visible, infrared (IR), and ultra-violet (UV) wavelengths from assets of interest. Other desirable properties for smokes and obscurants include being cheaply manufactured, easily deployable, indefinitely stable in storage, and environmentally benign. Currently, brass particles are being used in smokes and obscurants; however, there are severe limitations to its effectiveness including agglomeration, cost, and toxicity to the environment.

Much attention has recently been given to the modification of mica, SiO_2, as a replacement technology. Surface modification of mica is used to obtain the desired optical properties as well as absorption of electromagnetic radiation. While mica particles are environmentally friendly and inexpensive the metallic chemicals used to dope the surface to obtain the desired characteristics are neither, hence a new, innovative approach to developing long term smokes and obscurants solutions is needed.

The objective of this study is to investigate other chemical candidates that can be used to develop effective smoke and obscurant technologies to protect a wide range of military assets deployed throughout the world.

MoS_2, molybdenite, is a naturally occurring compound found in copper deposits that is known to exist in three different polymorphs: 2H, 1T, and 3R, see figure 1.[1] Table 1

summarizes the structural properties of MoS_2. 3R is uncommon and is not relevant to the present discussion.
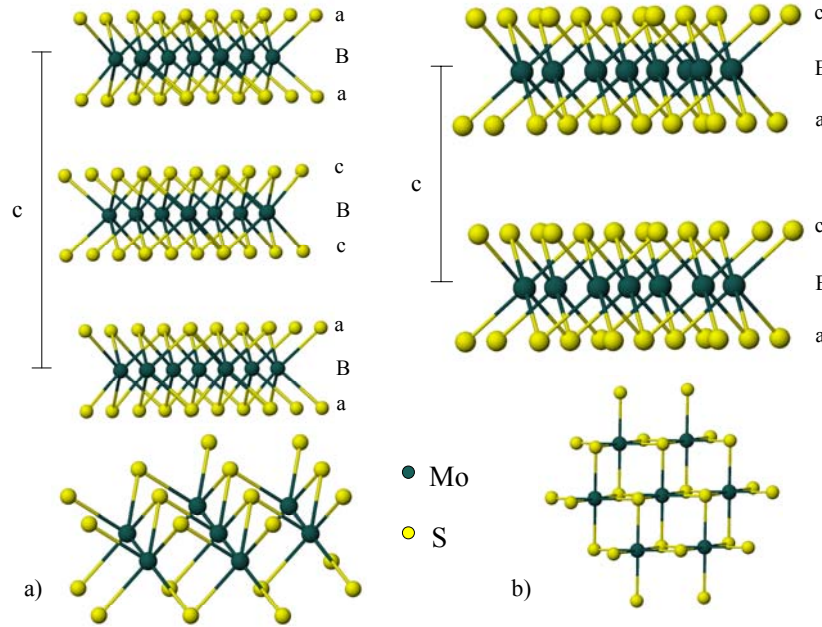
Figure 1. **Ball-and-stick drawing of (a) 2H-MoS$_2$ and (b) 1T-MoS$_2$. The color scheme is as follows: molybdenum, green; sulfur, yellow.**

MoS_2 intercalation chemistry has received considerable attention recently because it is known to undergo a structural change from the 2H to 1T polymorph when intercalated with lithium due to an electron transfer. 2H-MoS_2 is indefinitely stable and is commercially available via inexpensive synthetic processes in micron size particles.

Table 1. Characteristics of MoS$_2$ Polymorphs.

	2H-MoS$_2$	1T-MoS$_2$
MoS$_6$ Coordination	Trigonal Prismatic	Octahedral
Crystal Symmetry	$P6_3/mmc$	$P3$
Magnetism	diamagnetic	paramagnetic
Mo oxidation	Mo(IV), d^2	Mo(IV), d^2
Conductivity	semiconductor	metallic

The structure of pristine 2H-MoS$_2$ has P6$_3$/*mmc* crystal symmetry where $a = b = 3.15$ Å; $c = 12.27$ Å.[2,3] The 2H-MoS$_2$ unit cell consists of two complete MoS$_2$ layers with an aBa ••• cBc repeat pattern in the *c* direction, which are held together by weak van der Waals forces. The lower case letters represent the sulfur layers and the uppercase letter represents the molybdenum layers.[4] 2H-MoS$_2$ is hexagonally close packed with molybdenum coordinated to six sulfur atoms with trigonal prismatic geometry. The 2H polymorph exhibits semiconductor behavior and can be modified by inserting foreign compounds into the interlayer spaces.

In contrast, the Mo − S coordination for metastable 1T-MoS$_2$ changes from trigonal prismatic to octahedral through simultaneous glide motion by the molybdenum and sulfur planes.[5] The change in geometry reduces the unit cell to one aBc layer.[6] The 1T-MoS$_2$ polymorph exhibits metallic behavior because there is no band gap. The structural transition significantly reduces the crystal symmetry from *P*6$_3$/*mmc* to *P*3.

MoS$_2$ is a versatile flat, high aspect ratio nanoparticle that can be used as a smoke and obscurant to absorb all types of electromagnetic radiation. A high aspect ratio material is a crystallite in which one dimension is significantly different than the other two dimensions. A characteristic of the high aspect ratio material is that the interparticle adhesive forces of MoS$_2$ are strong enough to cause the dispersed MoS$_2$ particles to quickly agglomerate, making it a poor smoke and obscurant. To explore solutions to prevent particle agglomeration, the intercalation of MoS$_2$ with organic molecules that thermodynamically decompose to evolve gas was investigated. Intercalation with organic compounds will allow the MoS$_2$ particles to maintain the characteristics of a high

aspect ratio but should reduce the cohesion forces so the MoS_2 particles can fully disperse.

Intercalation chemistry is the process of reversibly inserting a guest molecule into a layered compound, referred to as the host. The insertion typically occurs in the van der Waals gap between the host layers. Schauffault first achieved intercalation with graphite as the host and sulfate as the guest in 1841.[6] The reaction is topotactic meaning the host structure remains unchanged by the intercalation. The chemical, electronic, and optical properties as well as the conductivity associated with intercalated compounds often significantly change, from the host's original properties, which has caused renewed interest in intercalation chemistry since the 1960's.[7] Chemists' ability to control these perturbations makes intercalation the focus of several research areas including catalysts, superconductors, and long term rechargeable batteries.[8-12] A wide range of guest species have been intercalated including; simple atomic species, alkali metals, polymers, and organometallics.[13] Lithium is commonly used as an electron donor, which causes the host material to be reduced. In the case of graphite, lithium intercalation causes the compound to become paramagnetic and experience a significant increase in conductivity in the direction perpendicular to the layers. Molybdenum oxide, nitrate ions, and hydrogen sulfate are commonly used as electron acceptor guest molecules.

Intercalation reactions can be concentration dependent in a phenomenon known as staging. At a high concentration the guest will intercalate in a well-ordered fashion between each host layer. As the intercalate concentration decreases, the intercalate will only fill every second layer, then every third layer, and so on until the concentration is too low to appreciably intercalate. [9,14] The initial degree of intercalation is measured by

comparing the lattice spacing of the pristine layered material with the new compound using XRD analysis. The increase in the lattice spacing indicates how the intercalate is most likely oriented within the host's framework, which is coupled with the area of the intercalate in the host framework to determine the maximum intercalate uptake.

Intercalation chemistry has been extensively studied and documented for a large number of transition metal dichalcoginides due to their potential for significant technological advances.[3,15,16] Transition metal dichalcoginides from group IV, V, and VI known as MX_2 compounds possess either a hexagonal or rhombohedral structure. Between the two X layers the metal atom occupies either a trigonal prismatic or an octahedral site. Typically, the M – X bonds are strong ionic or polar covalent bonds while the layers are held together by weak van der Waals forces.[3] The weak interlayer forces are exploited during intercalation. It has been well documented that most MX_2 systems undergo a charge transfer upon intercalation.[17] The addition or removal of an electron to the empty or partially filled band can invoke physical property changes in the host material depending on the guest – host interaction. Host materials have been reported to exhibit conductivity changes including; metallic to insulator, semiconductor to metallic, insulator to semiconductor, paramagnetic to diamagnetic, or diamagnetic to paramagnetic.[6] For example, ZrS_2, which is a semiconductor, can easily be altered to exhibit either insulator or metallic behavior depending on the guest intercalate.[18] Other examples include cobaltocene which loses its magnetic moment upon intercalation into TaS_2, and chromocene, which becomes paramagnetic upon TaS_2 intercalation.[6]

MX_2 compounds can exist in different forms known as polymorphs and can undergo further structural changes upon intercalation. This will be discussed in detail later. MS_2

and MSe_2 compounds have been found to make the most stable intercalate compounds while MTe_2 compounds have been found to be considerably unstable. Overall compound stability as well as intercalate uptake are dependent on the interaction between the host and guest molecules. On the other hand, interlayer expansion is only dependant on the intercalates size and orientation within the host lattice.[6]

Molybdenite cannot be directly intercalated with large guest molecules because it has a low electron affinity making it difficult to reduce. Therefore MoS_2 can only react with guests with low ionization potentials whose donated electron can occupy electronic levels above the bandgap.[4] Due to the difficulty in intercalating MoS_2 far fewer cases have been documented compared to $NbSe_2$ and other easily intercalated metal dichalcogenides.[19]

$2H$-MoS_2 reacts with n-butyl lithium to achieve a stoichometric product $LiMoS_2$ according to eq. 1.[20]

$$MoS_2 + n\text{-BuLi} \rightarrow LiMoS_2 + \tfrac{1}{2} C_4H_{10} + \tfrac{1}{2} C_4H_8 \qquad (1)$$
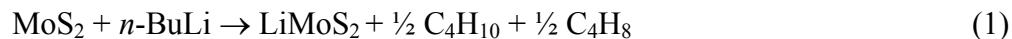
$LiMoS_2$ adopts the $1T$-MoS_2 structure with P3 crystal symmetry where $a = b = 3.360$ Å and $c = 6.311$ Å.[5,21] A ball-and-stick drawing of this structure is given in figure 2.
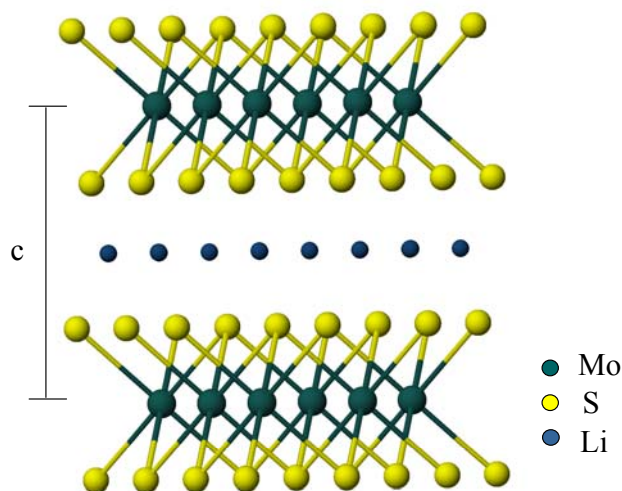
Figure 2. **Ball-and-stick drawing of LiMoS$_2$ structure perpendicular to the c axis.** **The coloring scheme is as follows: molybdenum, green; sulfur, yellow; lithium, purple.**

The distinct expansion of the *c* parameter is due to lithium intercalation into the van der Waals gap between the sulfur layers. The lithium resides in octahedral holes formed by the MoS$_2$ layers.[17,22]

The density of states diagram in figure 3, shows how one additional electron from lithium will effect the 2H and 1T structures. The extra electron goes into the metal's d orbital and molybdenum is consequently reduced from Mo^{+4} (d^2) to Mo^{+3} (d^3). The significant increase in electronic energy in 2H-MoS$_2$ due to the large bad gap creates instability in the trigonal prismatic coordination. The 1T polymorph experiences a slight increase in electronic energy upon the addition of the electron, but is by far more stable than the 2H polymorph. This difference in stability is the driving force for the structural change from 2H to 1T.[5]
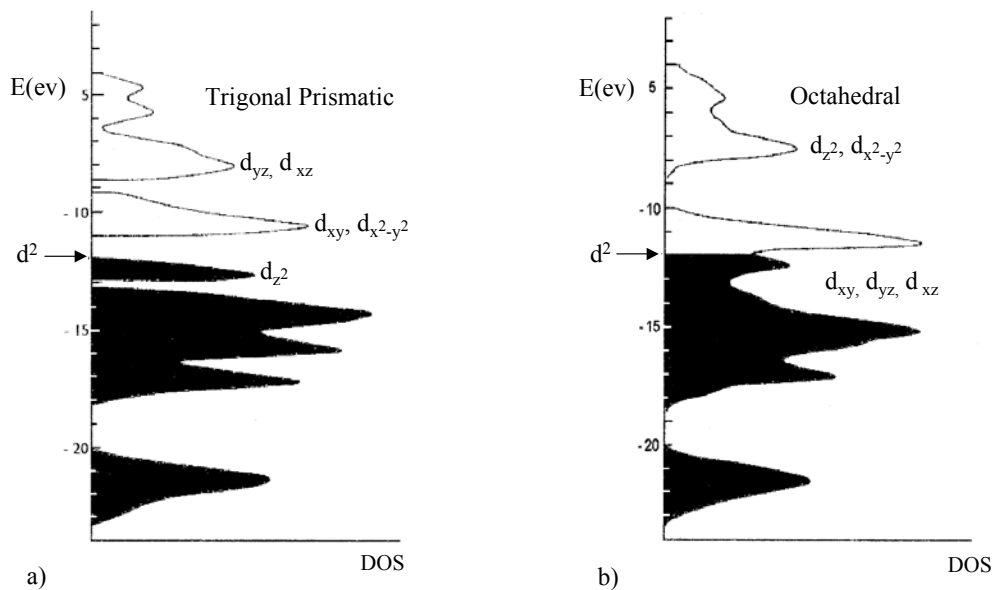
Figure 3. Comparison of d-band density of states for a) 2H-MoS$_2$ and b) 1T-MoS$_2$.[23] The shaded area indicates the states occupied by MoS$_2$.

The change from semiconductor for 2H-MoS$_2$ to metallic for 1T-MoS$_2$ has an important effect on the optical properties. 2H-MoS$_2$ will not be able to absorb all types of radiation because the extra energy has to increase approximately 1 eV above the Fermi level to reach an allowed transition.[24] This jump makes the 2H polymorph vulnerable to penetration by low energy radiation sources such as infrared. The 1T-MoS$_2$ polymorph however, has a continuum of states that are empty above the Fermi level making all transitions allowed when the compound is exposed to radiation.

The 1T-MoS$_2$ structure shows an increased affinity for intercalation and remains in the octahedral geometry until the intercalate is removed by heating or aging.[25] Potential organic intercalates cannot simply diffuse into the MoS$_2$ layers. Instead a two-step exfoliation and reflocculation process is needed to intercalate foreign compounds.

Upon the addition of excess water, hydrogen gas formation forces the MoS$_2$ layers apart generating exfoliated MoS$_2$ (eq. 2). In this state, the single MoS$_2$ layers are

suspended in the aqueous solution and the majority of lithium ions are removed as lithium hydroxide. It has been well documented that approximately 10 % of the lithium remains intercalated in the MoS_2 layers.[7]

$$LiMoS_2 + H_2O \rightarrow LiOH_{(aq)} + \tfrac{1}{2}H_{2(g)} + Li_{0.1}MoS_{2\ (exfoliated)} \qquad (2)$$
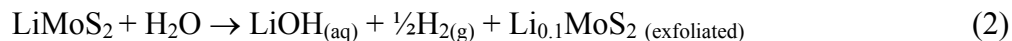
The structure of single layer MoS_2 has been extensively studied.[25] XRD analysis shows only (hk0) reflections consistent with a single layer material. A distorted $2a_o$ x $2a_o$ superlattice was determined by the presence of intense (210), (300), (320), and (410) reflections. These reflections were used to calculate an a_o value of 3.27 Å which is a 3.5 % increase from pristine MoS_2. The geometry of single layer MoS_2 was determined by modeling the XRD patterns of trigonal prismatic and octahedral single layer MoS_2. The experimental (100) reflection was found to match the calculated octahedral (100) reflection exactly thus confirming the octahedral geometry.[26] The addition of an aqueous solution of intercalate causes the exfoliated MoS_2 layers to reflocculate hence sandwiching the intercalate between the layers (eq. 3).

$$Li_{0.1}MoS_{2\ (exfoliated)} + organic \rightarrow Li_{0.1}MoS_2(organic)_{x\ (reflocculated)} \qquad (3)$$

A wide variety of materials have been successfully intercalated into MoS_2 using the exfoliation - reflocculation process including; amines, polymers, and organometallics.[7,15,27-30] Well characterized examples include a series of secondary amines and a series of tetraazamacromolecules which are reported to intercalate parallel to the MoS_2 layers.[31,32] The intercalated compounds experience a trend of decreasing intercalate uptake as the size of the guest molecule increases.[28] Naphthalene has also been reported as a MoS_2 intercalate.[33] Again the guest intercalates parallel to the MoS_2 host layers however the molar ratio of naphthalene can be controlled by varying the

stirring times. Like most intercalated MoS_2 compounds the guests are weakly

intercalated and will decompose upon heating or aging.

This research focuses on the intercalation of three "gas-forming" organic molecules;

ethyl diazoacetate (EDA), diethyl oxalate (DEO) and Meldrum's Acid (MA) into MoS_2

(figure 4).
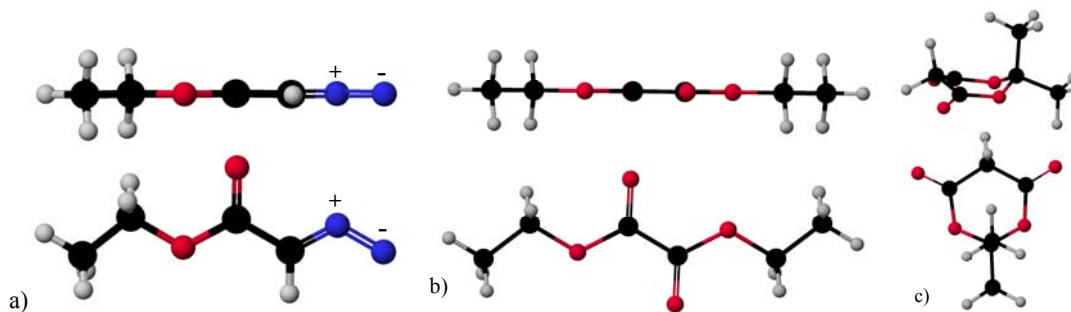
Figure 4. Ball-and stick drawing of the organics used for intercalation (a) ethyl diazoacetate (EDA) (b) diethyl oxalate (DEO) and (c) Meldrum's acid (MA). The color scheme is as follows: carbon, black; hydrogen, gray; oxygen, red; nitrogen, blue.

We propose that large volumes of gas will form in the interparticle space of the MoS_2

upon heating, which causes exfoliation and dispersion of the nanoparticles particles into

the air according to scheme 1.

Scheme 1. Proposed Reaction Mechanism for Dispersed MoS_2 particles.
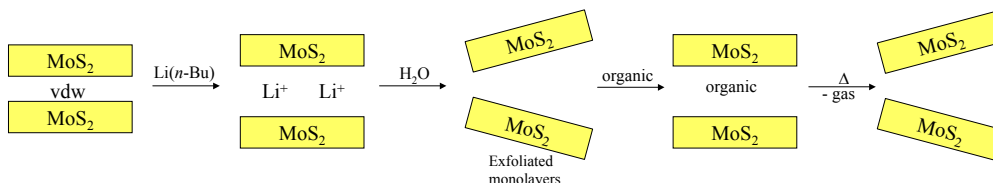
The expected products of thermal decomposition are carbon dioxide, nitrogen, ethane,

and ethylene gas. The gases are environmentally friendly and non-toxic. Likewise, the

dispersed MoS_2 particles, which revert to the 2H-MoS_2 polymorph, are not harmful once

they have settled on the ground.

Experimental Section

General Information. Standard Schlenk techniques were used for all air-sensitive

solution processes. All chemicals were purchased from Aldrich and used as received.

The purity of EDA, DEO, and MA was confirmed by NMR and IR. Deionized water was

degassed for 15 minutes prior to addition to the reaction mixture.

X-ray diffraction (XRD) patterns were recorded using a Bruker C2 Discover X-ray

powder diffractometer with a HiStar area detector and Cu Kα radiation. Typically, six

300 second frames were collected and merged to give 2θ scans from 4° to 90°. Unit cell

indexing was performed using MDI Jade software.[34] The air sensitive compound,

$LiMoS_2$, was wrapped in saran wrap in a drybox before XRD. Thermogravimetric

analysis (TGA) of samples was carried out using a TA instruments Q Series 500 with an

autosampler. A typical run consisted of an approximately 40 mg powder sample in a

platinum pan with a temperature ramp to 600 °C at 2 °C/min. The experiments were

done under air and nitrogen to determine the temperature of MoS_2 reformation and the

thermal decomposition pathways in different environments. Microanalysis was

performed by Atlantic Microlabs, Inc., Norcross, Georgia for carbon, hydrogen, and

nitrogen content. Infrared Spectroscopy (IR) was performed using a diffuse reflectance

accessory and a liquid crystal cell on a Thermo Nicolet Nexus 670 FT-IR ESP

Spectrometer. [1]H Nuclear Magnetic Resonance (NMR) spectra were collected on a

Bruker DRX400 spectrometer at 400 MHz. D-Chloroform ($CDCl_3$; 7.24 ppm) was used

as the reference solvent in the ^{1}H NMR. Differential Scanning Calorimetry (DSC) was

carried out using a TA instruments Q1000 with an autosampler. The instrument has a

temperature range of −90 °C to 725 °C. In a typical experiment, approximately 10 mg of

sample was loaded into a platinum pan and then heated to 300 °C ($T_{ramp} = 5$ °C or 10 °C/min). An empty platinum pan was used as a reference.

Synthesis. Preparation of LiMoS$_2$. Slight modifications of previously reported methods were used to prepare LiMoS$_2$.[21,35,36] In a schlenk flask an approximate 10 fold molar excess of 1.6 M solution of *n*-butyl lithium in hexanes (5 mL, 53.1 mmol) was added to MoS$_2$ (1.0 g, 6.25 mmol) producing a black solution. The reaction mixture was stirred for 48 hours. Excess *n*-butyl lithium was removed by cannulation. LiMoS$_2$ was washed with hexane and dried under vacuum for 36 hours.

Preparation of MoS$_2$ – EDA product. EDA (2.6 mL, 25 mmol) was dissolved in 10 mL ethanol/water (1:1) solution. The aqueous organic solution was added to LiMoS$_2$ (1.0 g, 6.22 mmol) via cannula. The black reaction mixture was stirred for 48 hours and then centrifuged. The supernatant was decanted and the black slurry was thoroughly dried in a dessicator. The dried product was a hard, black solid.

Preparation of Li$_{0.1}$MoS$_2$(DEO)$_{0.10}$. DEO (3.4 mL, 25 mmol) was dissolved in 10 mL ethanol/water (1:1) solution. The aqueous organic solution was added to LiMoS$_2$ (1.0 g, 6.22 mmol) via cannula. The black reaction mixture was stirred for 48 hours and then centrifuged. The supernatant was decanted and the black slurry was thoroughly dried in a dessicator. The dried product was a hard, black solid.

Preparation of Li$_{0.1}$MoS$_2$(MA)$_{0.14}$. MA (3.60 g, 25 mmol) was dissolved in 10 mL acetonitrile/water (1:1) solution. The aqueous organic solution was added to LiMoS$_2$ (1.0 g, 6.22 mmol) via cannula. The black reaction mixture was stirred for 48 hours and then centrifuged. The supernatant was decanted and the black slurry was thoroughly dried in a dessicator. The dried product was a hard, black solid.

Preparation of $Li_{0.1}MoS_2(H_2O)_x(EtOH)_y$. 20 mL of water were added to $LiMoS_2$ and then sonicated 3 hours. The black reaction mixture was centrifuged. The compound was washed twice with ethanol and water. The supernatant was decanted and the solid was thoroughly dried in a dessicator. The dried product was a hard, black solid.

TGA Analysis. The reported concentration of the organic was calculated from the TGA data run in the air where the final product was MoO_3 (XRD analysis). The number of moles of molybdenum in MoO_3 equals the number of moles of molybdenum in the intercalated compounds. The number of moles of molybdenum in MoO_3 is then used to calculate a known starting mass of $Li_{0.1}MoS_2$ without the organic component. The difference between the starting material (less the mass attributed to water and ethanol) and the mass of the $Li_{0.1}MoS_2$ is the mass of the organic present in the intercalated compound, which is converted to moles of organic intercalate. The concentration organic intercalate is the ratio of moles of organic intercalate to moles of $Li_{0.1}MoS_2$.

Results

$Li_{0.1}MoS_2(organic)_x$. The "gas forming" organic compounds, diethyl oxalate (DEO) or Meldrum's Acid (MA), react with the exfoliated MoS_2 suspension to form the intercalated compounds $Li_{0.1}MoS_2(DEO)_{0.10}$ and $Li_{0.1}MoS_2(MA)_{0.14}$, respectively. (See equations 4 and 5). Ethyl diazoacetate does not intercalate into MoS_2 under identical conditions, but the product isolated from this reaction will be referred to as $Li_{0.1}MoS_2 -$ EDA product.

$$Li_{0.1}MoS_{2\,(exfoliated)} + 4\,DEO \rightarrow Li_{0.1}MoS_2(DEO)_{0.10} \tag{4}$$

$$Li_{0.1}MoS_{2\,(exfoliated)} + 4\,MA \rightarrow Li_{0.1}MoS_2(MA)_{0.14} \tag{5}$$

The black intercalated compounds are thermally sensitive, decompose in air, and have been characterized by X-ray diffraction (XRD), thermogravimetric analysis (TGA), ^{1}H nuclear magnetic resonance (NMR), differential scanning calorimetry (DSC), and elemental analysis (EA).

The concentration of the organic in the intercalated compound was calculated using air TGA data. Complete decomposition of the intercalated compound to MoO_3 in TGA experiments run in air allowed for the determination of the intercalate concentration based on molar ratio of molybdenum. Nitrogen TGA, XRD, and NMR support the calculated concentration and will be discussed later.

In this study, $Li_{0.1}MoS_2(H_2O)_x(EtOH)_y$ is used as a reference and compared to the other intercalated compounds. For the synthesis of $Li_{0.1}MoS_2(H_2O)_x(EtOH)_y$, an excess of water was reacted with the MoS_2 suspension causing reflocculation of the MoS_2 layers and intercalation of the water molecules. Subsequent washing with ethanol displaced some of the water molecules resulting in a mixture of intercalated water and ethanol. Molar ratio determinations for water and ethanol in this compound were impossible due to the presence of two intercalates that could not be distinguished in characterization data.

XRD. The results of the XRD analysis for the intercalated compounds are shown in figure 5 and summarized in table 2. The XRD profiles of MoS_2 and $LiMoS_2$ are shown in figure 6 for reference.
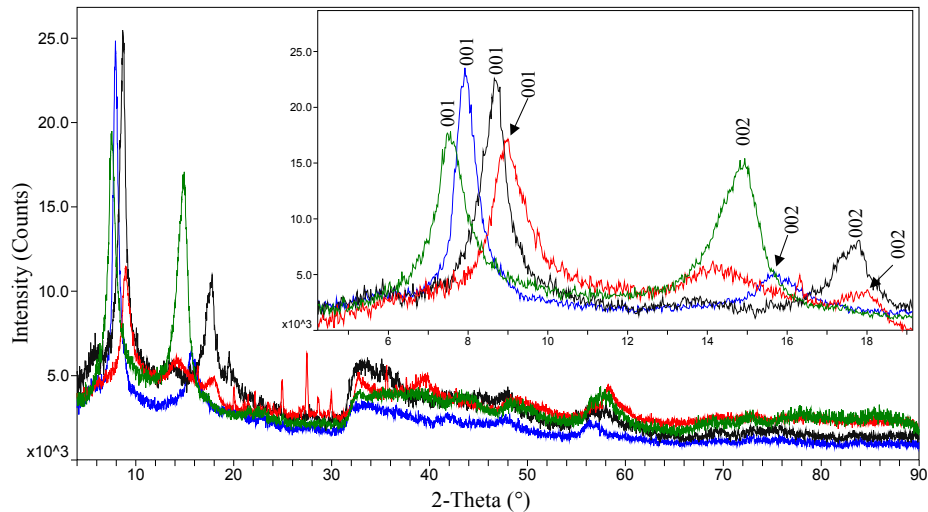
Figure 5. XRD patterns of: $Li_{0.1}MoS_2$ – EDA product (blue) $Li_{0.1}MoS_2(DEO)_{0.10}$ (black), $Li_{0.1}MoS_2(MA)_{0.14}$ (red), $Li_{0.1}MoS_2(H_2O)_x(EtOH)_y$ (green). The inset shows the region from $2\theta = 4\text{-}20°$ in more detail.
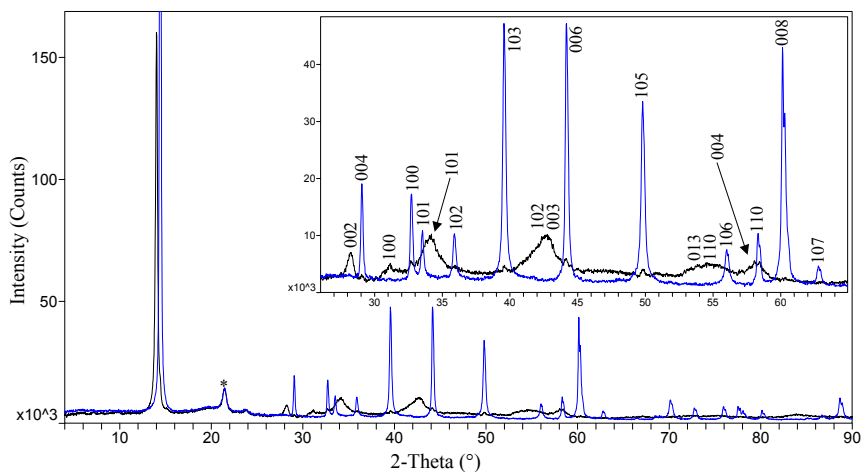
Figure 6. XRD pattern of pristine MoS_2 (blue) and $LiMoS_2$ (black). The inset shows the region from $2\theta = 26\text{-}65°$ in more detail. The asterisk denotes the reflection due to saran wrap impurities.

The intercalated compounds are best characterized by the shift in the (001) reflections seen in the XRD analysis (figure 6). The increase from 6.15 Å for pristine $2H\text{-}MoS_2$ to 11.15 Å, 10.20 Å, and 9.97 Å for the $Li_{0.1}MoS_2$ – EDA compound, $Li_{0.1}MoS_2(DEO)_{0.10}$, and $Li_{0.1}MoS_2(MA)_{0.14}$, respectively, indicates that guest materials have been intercalated

15

into the interlayer space of MoS_2. The reference compound, $Li_{0.1}MoS_2(H_2O)_x(EtOH)_y$ has an interlayer increase of 5.53 Å to 11.68 Å.

Table 2. Summary of Results from Intercalation of Organic Guest Material

Intercalated Compound	c (Å)	Δc Lattice Expansion (Å)[a]	Guest/Host x (mol/mol)[b]	Maximum guest/host x (mol/mol)[c]
$LiMoS_2$	6.31	0.16	1	1
$Li_{0.1}MoS_2$ - EDA product	11.15	5.00	0.00	0.21
$Li_{0.1}MoS_2(DEO)_{0.10}$	10.20	4.05	0.10	0.16
$Li_{0.1}MoS_2(MA)_{0.14}$	9.97	3.82	0.14	0.14
$Li_{0.1}MoS_2(H_2O)_x(EtOH)_y$	11.68	5.53		

a - Difference between the intercalated compound lattice expansion (c) and 2H-MoS (6.15 Å)

b - Concentration of organic calculated by air TGA

c - Maximum possible concentration based on organic orientation (parallel to MoS_2 layers)

TGA. TGA was used to determine both the concentration of the intercalate and the temperature of deintercalation. Thermal deintercalation of the organic guest results in the reformation of MoS_2 and is dependant on the organic intercalate. The results of the TGA experiments are shown in figures 7 and 9 and summarized in tables 3, 4, and 5.

To verify if the EDA, DEO, or MA was present in the intercalated compound, the thermal behavior of the intercalated compound was compared to the standards, MoS_2 and $Li_{0.1}MoS_2(H_2O)_x(EtOH)_y$ in both air and nitrogen. The first observed mass loss for the intercalated compounds is attributed to dehydration. Dehydration has been reported to occur within a range of temperatures for disulfide compounds, from ambient temperature to approximately 80 °C, depending on the intercalate.[37,38] Thermal decomposition at temperatures greater than 300 °C and after the reformation of MoS_2 in air or nitrogen, is attributed to the oxidation of MoS_2 and is not discussed in this study.

Figure 7 shows the observed nitrogen TGA curves and the decomposition results are summarized in table 3. The concentration of the organic in the intercalated compound

was calculated from the nitrogen TGA data and is in good agreement with the

concentration calculated from the air TGA data. The difference between the mass of the

starting material (less the mass attributed to water) and the mass of $Li_{0.1}MoS_2$ is equal to

the mass of organic present in the intercalated compound. The concentration of organic

intercalated in both the DEO and MA compounds (ratio of moles of organic intercalate to

moles of $Li_{0.1}MoS_2$) yielded 0.15, a value consistent with those calculated for DEO and

MA from air TGA data (0.10 and 0.14, respectively).
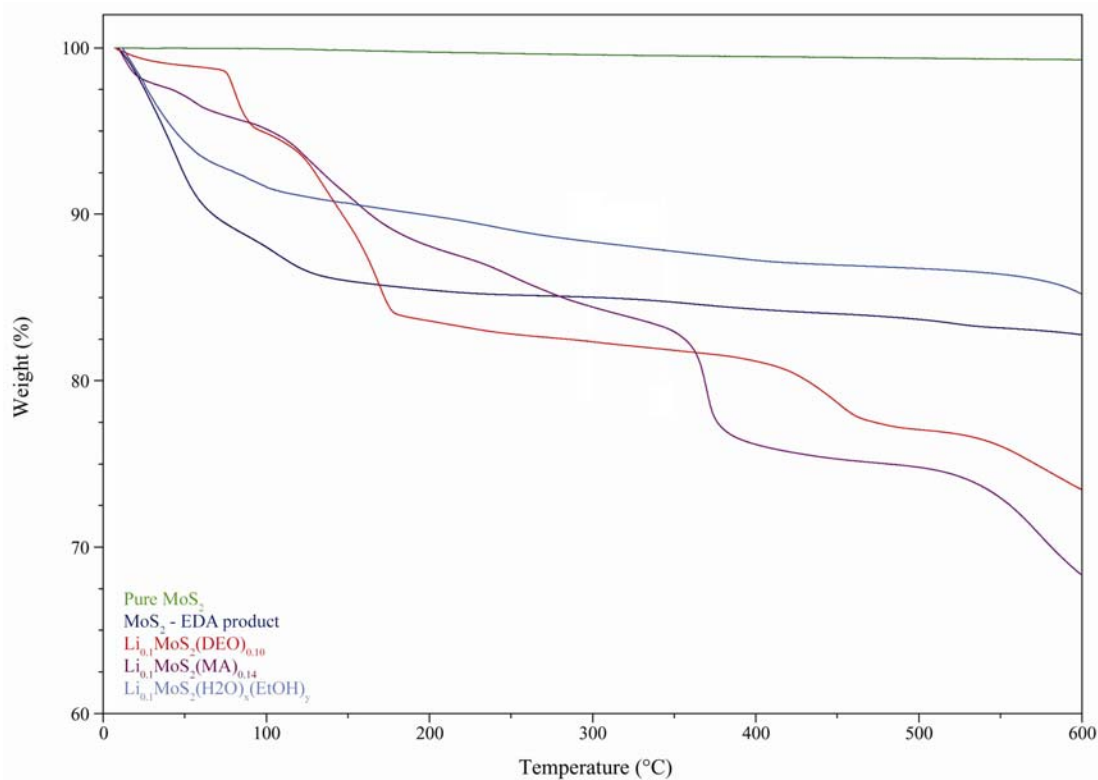
Figure 7. TGA curves under a nitrogen environment of: pristine 2H-MoS₂ (green), Li₀.₁MoS₂ – EDA product (dark blue), Li₀.₁MoS₂(DEO)₀.₁₀ (red), Li₀.₁MoS₂(MA)₀.₁₄ (purple), and Li₀.₁MoS₂(H₂O)ₓ(EtOH)ᵧ (bright blue)

In a nitrogen environment, pristine 2H-MoS₂ experienced minimal mass loss at

temperatures above 600 °C and XRD analysis indicates that 2H-MoS₂ is unchanged.

However, the intercalated compounds thermally decompose in a multi-step process to

MoS$_2$ and Li$_2$MoO$_4$ when heated to 600 °C, as determined by XRD.

Li$_{0.1}$MoS$_2$(H$_2$O)$_x$(EtOH)$_y$ decomposes in a single 11.6 % mass loss, attributed to the

thermal decomposition of water and ethanol, to Li$_{0.1}$MoS$_2$ at 25.7 °C. The Li$_{0.1}$MoS$_2$ -

EDA product experiences an immediate 13.3 % mass loss at 43.8 °C attributed to the

thermal decomposition of water and ethanol similar to the results observed in

Li$_{0.1}$MoS$_2$(H$_2$O)$_x$(EtOH)$_y$. No other mass loss is observed in the Li$_{0.1}$MoS$_2$ – EDA

product suggesting that no EDA is present in the intercalated compound.

Li$_{0.1}$MoS$_2$(DEO)$_{0.10}$, has a 5.1 % mass loss due to dehydration at 80.6 °C. The mass loss

is followed by an 11.4 % mass loss at 135.0 °C attributed to the thermal decomposition of

the intercalated compound by the sublimation of the DEO intercalate. Li$_{0.1}$MoS$_2$(MA)$_{0.14}$

experiences a 4.3 % mass loss at 55.9 °C due to dehydration of water in the sample. The

subsequent 11.3 % mass loss at 124.1 °C is attributed to the sublimation of the MA

intercalate from the intercalated compound.

<p style="text-align:center">Table 3.   Summary of Results from TGA Experiments in Nitrogen</p>

Intercalated Compounds	Percentage Mass Loss in Nitorgen (%)	Onset Temp in Nitrogen (°C)[a]	First Derivative Temp (°C)[b]	Compounds Lost
Li$_{0.1}$MoS$_2$ - EDA product	13.3	23.5	43.8	H$_2$O/EtOH
Li$_{0.1}$MoS$_2$(DEO)$_{0.10}$	5.12	75.8	80.6	H$_2$O/EtOH
	11.4	133.1	135.0	DEO
Li$_{0.1}$MoS$_2$(MA)$_{0.14}$	4.3	46.5	55.9	H$_2$O/EtOH
	11.3	107.7	124.1	MA
Li$_{0.1}$MoS$_2$(H$_2$O)$_x$(EtOH)$_y$	11.6	30.9	25.7	H$_2$O/EtOH

a - intersection of tangent lines
b - Temperature at maximum rate of weight loss

A consistent mass loss in all nitrogen TGA curves at approximately 575 °C is due to

oxygen reacting with MoS$_2$ and residual lithium to give Li$_2$MoO$_4$ as determined by XRD

(figure 8). The source of the oxygen for MoS$_2$ oxidation is most likely from water or

ethanol in the compound. The amount of lithium remaining in the intercalated

compounds is determined by comparing the experimental relative intensities of MoS_2 and Li_2MoO_4 observed in the XRD pattern. The ratio of Li_2MoO_4 to MoS_2 was determined to be approximately 1:19 or approximately 5 %. Therefore the initial lithium concentration was calculated to be approximately 0.1, consistent with the literature reports.[7]
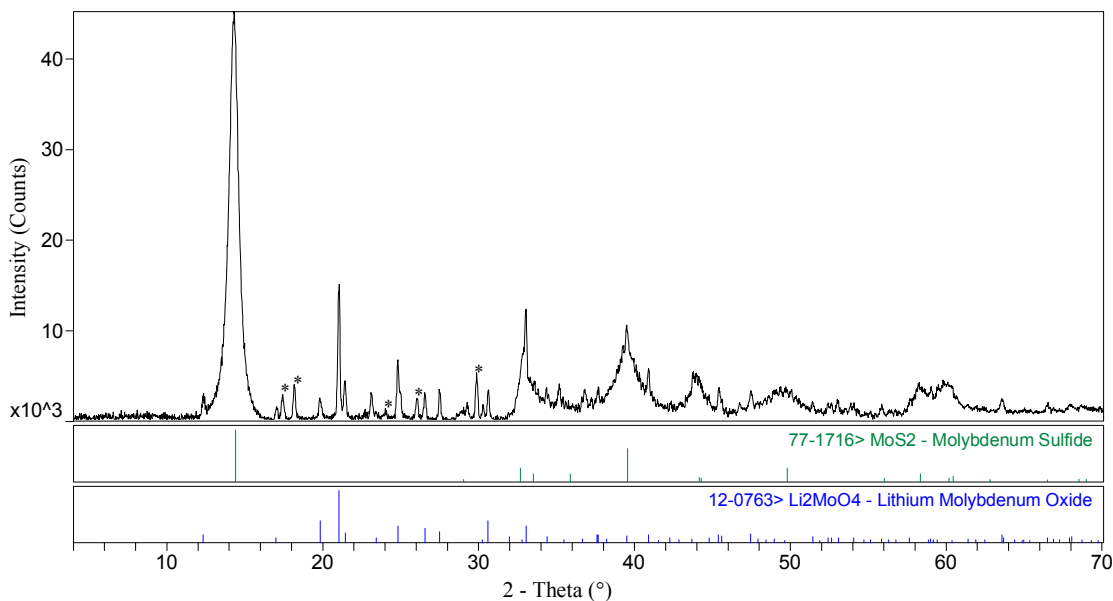
Figure 8. XRD pattern of the decomposition product of $Li_{0.1}MoS_2(DEO)_{0.10}$ after TGA experiment in nitrogen to 600°C. The asterisks denote impurities due to SiO_2.

The air TGA curve is seen in figure 9 and a summary of the decomposition data is shown in table 4. In high temperature air TGA experiments, pristine $2H$-MoS_2 and the intercalated compounds decompose to single phase MoO_3. Presumably, lithium sublimes out of the intercalated compound due to its high volatility in oxygen.
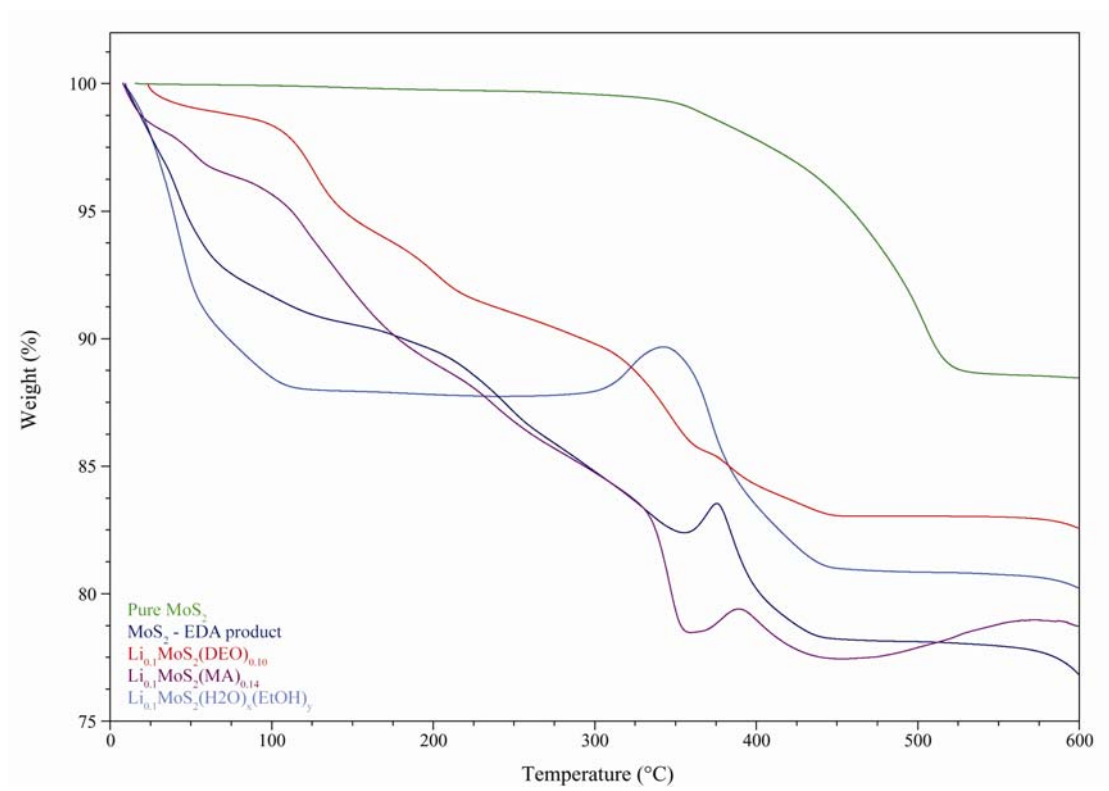
Figure 9. TGA curves in an air environment of: pristine 2H-MoS$_2$ (green), Li$_{0.1}$MoS$_2$ – EDA product (dark blue), Li$_{0.1}$MoS$_2$(DEO)$_{0.10}$ (red), Li$_{0.1}$MoS$_2$(MA)$_{0.14}$ (purple), and Li$_{0.1}$MoS$_2$(H$_2$O)$_x$(EtOH)$_y$ (bright blue)

Li$_{0.1}$MoS$_2$(H$_2$O)$_x$(EtOH)$_y$ decomposes to MoS$_2$ in a single 12.1 % mass loss, due to

the deintercalation of water and ethanol, at 41.6 °C. Similarly, the Li$_{0.1}$MoS$_2$ – EDA

product shows a single 10.2 % mass loss at 43.2 °C. No other mass loss is observed

substantiating the results from the nitrogen TGA experiments that EDA is not intercalated

into MoS$_2$. Li$_{0.1}$MoS$_2$(DEO)$_{0.10}$ showed an immediate 1.3 % mass loss at 23.4 °C

attributed to dehydration. The mass loss was followed by a 7.6 % mass loss at 127.1 °C

attributed to the decomposition of the intercalated compound by sublimation of the DEO

intercalate. A 3.5 % mass loss attributed to the deintercalation of water was observed at

52.2 °C for Li$_{0.1}$MoS$_2$(MA)$_{0.14}$. Dehydration is followed by an 11.1 % mass loss at 121.8

°C which is attributed to the thermal decomposition of the intercalated compound by

sublimation of the MA intercalate.

Table 4. Summary of Results from TGA Experiments in Air

Intercalated Compounds	Percentage Mass Loss in Air (%)	Onset in Air (°C)[a]	First Derivative Temp (°C)[b]	Compounds Lost
MoS_2	11.5	404.1	503.3	MoS_2 oxidation
$Li_{0.1}MoS_2$ - EDA product	10.2	38.5	43.2	H_2O/EtOH
$Li_{0.1}MoS_2(DEO)_{0.10}$	1.28	25.0	23.4	H_2O/EtOH
	7.6	109.8	127.1	DEO
$Li_{0.1}MoS_2(MA)_{0.14}$	3.53	42.7	52.2	H_2O/EtOH
	11.1	104.6	121.8	MA
$Li_{0.1}MoS_2(H_2O)_x(EtOH)_y$	12.1	26.0	41.6	H_2O/EtOH

a - Temperature determined

b - temperature at greatest rate of mass loss occurs

As previously discussed, the reported concentration of DEO and MA in the intercalated compounds (0.10 and 0.14, respectively) was based on the complete decomposition of the intercalated compound to the fully oxidized product, MoO_3, as determined by XRD (figure 10).
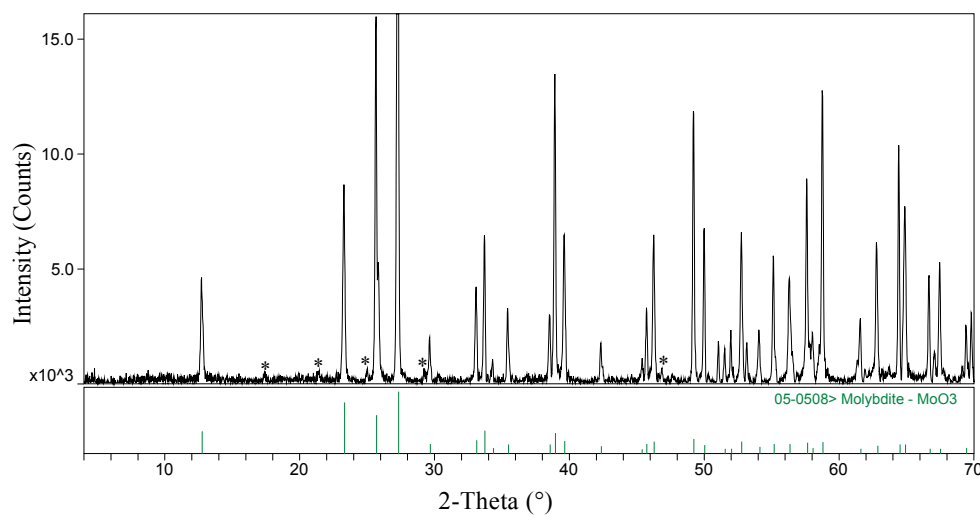
Figure 10. XRD pattern of the decomposition product of $Li_{0.1}MoS_2(DEO)_{0.10}$ after TGA experiment in air to 600°C. The asterisks denote impurities due to SiO_2.

¹H NMR. The $Li_{0.1}MoS_2 - EDA$ product, $Li_{0.1}MoS_2(DEO)_{0.10}$, $Li_{0.1}MoS_2(MA)_{0.14}$,

and $Li_{0.1}MoS_2(H_2O)_x(EtOH)_y$ were individually soaked in a $CDCl_3$ solution in an effort to

extract the intercalate from the MoS_2 layers. Approximately a 10 fold excess of

naphthalene, to the concentration of intercalated organic, was added to the $CDCl_3$

solution to use as an internal standard. A ¹H NMR of the resulting solution shows peaks

that correspond to the intercalated material. There are intense water and grease peaks

present at 1.52 and 0.86 ppm respectively. The water was attributed to both $CDCl_3$

solvent and the intercalated compound.

The NMR of $Li_{0.1}MoS_2 - EDA$ product (figure 11) showed water and trace amounts

of ethanol (see inset). The NMR data shows that no EDA was extracted from the

intercalated compound, possibly indicating that no EDA was present, consistent with

TGA data.
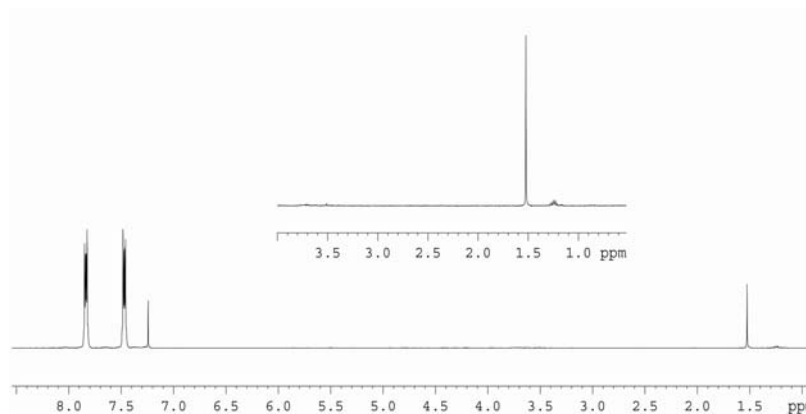
Figure 11. NMR spectra of $Li_{0.1}MoS_2$ – EDA product in $CDCl_3$. The inset shows the region from 0.5 – 4.0 ppm in more detail.

Intense peaks at 1.37 and 4.36 ppm in the NMR of $Li_{0.1}MoS_2(DEO)_{0.10}$ are attributed

to DEO (figure 12). The integral ratio of the ethyl groups to the naphthalene standard

was used to calculate a DEO concentration of 0.12, which is consistent with 0.10 relative

to air TGA data. After the NMR experiment, complete decomposition of

Li$_{0.1}$MoS$_2$(DEO)$_{0.10}$, observed by XRD analysis, results in the formation of amorphous

MoS$_2$ suggesting that all of the DEO was extracted from the MoS$_2$ layers.
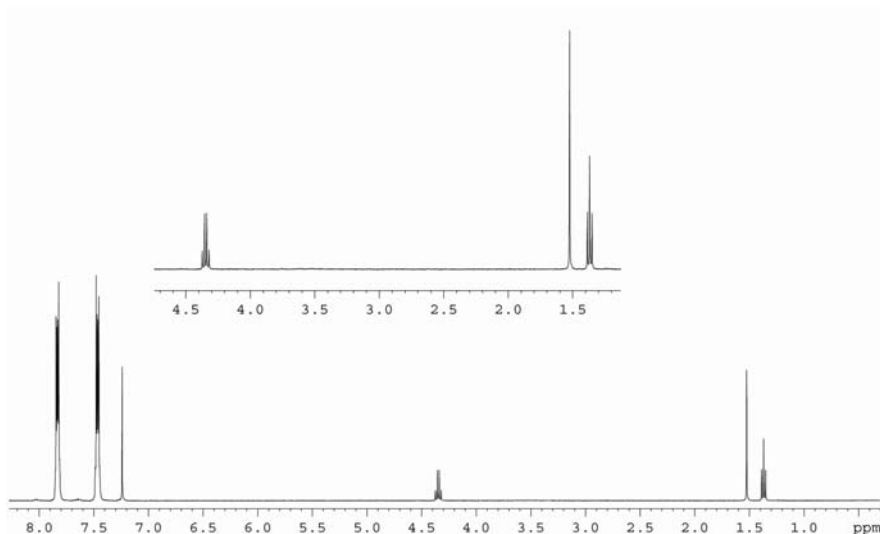
Figure 12. NMR spectra of Li$_{0.1}$MoS$_2$(DEO)$_x$ in CDCl$_3$. The inset shows the region from 1.2 – 4.5 ppm in more detail.

Two singlets at 1.77 and 3.60 ppm attributed to Meldrum's acid are observed in the

NMR of Li$_{0.1}$MoS$_2$(MA)$_{0.14}$ (figure 13). The integral ratio of the methylene group and

the methyl groups to the naphthalene standard results in a molar ratio of 0.06 for

Meldrum's Acid, approximately half of the concentration calculated by the TGA results

(0.14). XRD analysis of the Li$_{0.1}$MoS$_2$(MA)$_{0.14}$ after the NMR experiment, showed a

decrease in MA peak intensity after soaking in the CDCl$_3$ solution, implying that total

MA extraction did not occur. Li$_{0.1}$MoS$_2$(MA)$_{0.14}$ was becoming more amorphous but had

not fully converted to MoS$_2$, therefore accounting for the low concentration of organic

intercalate determined by NMR, suggesting that Li$_{0.1}$MoS$_2$(MA)$_{0.14}$ is a more robust

compound than Li$_{0.1}$MoS$_2$(DEO)$_{0.10}$.
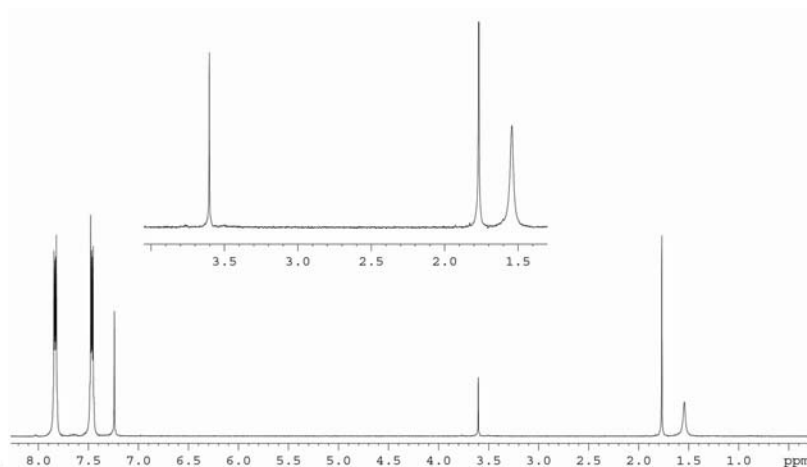
Figure 13. NMR spectra of Li$_{0.1}$MoS$_2$(MA)$_x$ in CDCl$_3$. The inset shows the region from 1.4 – 4.0 ppm in more detail.

As expected, water and ethanol peaks were observed in the NMR of

Li$_{0.1}$MoS$_2$(H$_2$O)$_x$(EtOH)$_y$ (figure 14). The presence of ethanol in the compound

demonstrates that the solvent is preferentially intercalated when the compound is washed.

Two singlets observed at 2.16 and 2.09 ppm are attributed to impurities in the NMR

sample. A complete reduction in peak intensity, observed by XRD analysis, resulting

from the formation of amorphous MoS$_2$ suggests that total extraction of water and

ethanol from the MoS$_2$ layers was achieved.
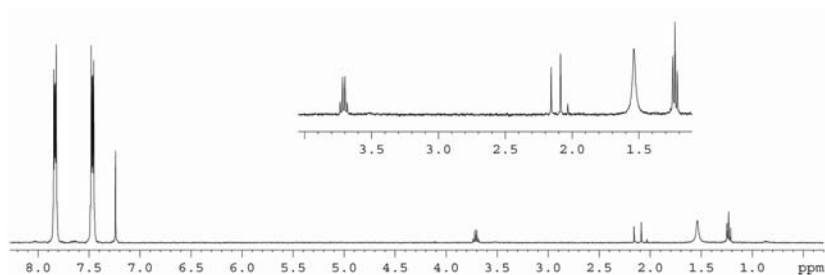
Figure 14. NMR spectra of Li$_{0.1}$MoS$_2$(H$_2$O)$_x$(EtOH)$_y$ in CDCl$_3$. The inset shows the region from 1.2 – 4.0 ppm in more detail.

DSC. The DSC traces are shown in figure 15 and the data is summarized in table 5. DSC is used to measure temperatures and heat flows associated with thermal transitions in a material. The endothermic temperatures observed in this study may be due to the $1T\text{-}MoS_2$ to $2H\text{-}MoS_2$ phase transition.
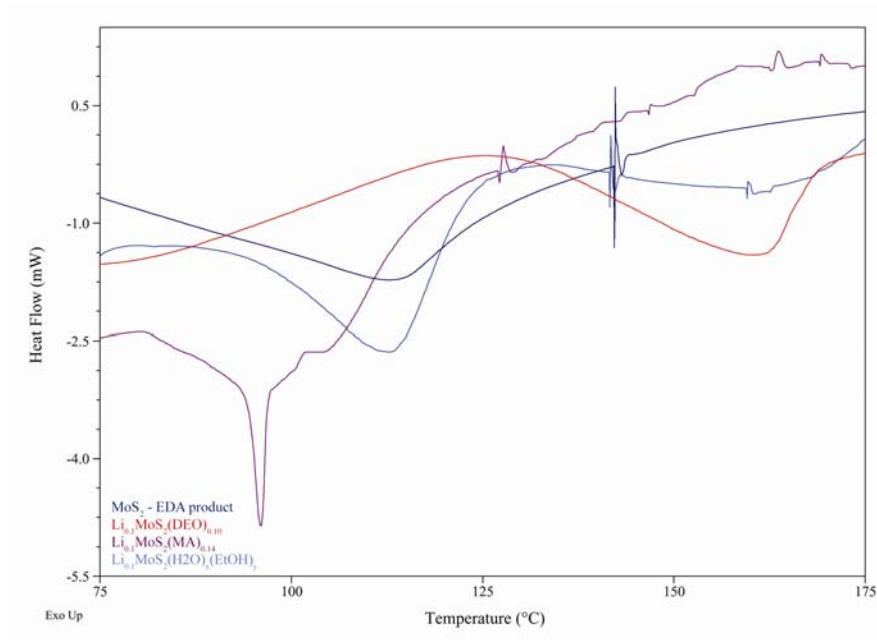
Figure 15. DCS traces in a nitrogen environment of: $Li_{0.1}MoS_2$ - EDA product$_x$ (dark blue), $Li_{0.1}MoS_2(DEO)_{0.10}$ (red), $Li_{0.1}MoS_2(MA)_{0.14}$ (purple), and $Li_{0.1}MoS_2(H_2O)_x(EtOH)_y$ (bright blue)

Table 5. Summary of DSC Results

Intercalated Compounds	Endothermic Peak Maximum (°C)[a]
$1T\text{-}MoS_2$	~100[b]
$Li_{0.1}MoS_2$ - EDA product	113
$Li_{0.1}MoS_2(DEO)_x$	160.3
$Li_{0.1}MoS_2(MA)_x$	95.9
$Li_{0.1}MoS_2(H_2O)_x(EtOH)_y$	112.7

a - Temperaure at which phase transition occurs
b - See Ref 8

An endotherm at ~100 °C has been documented for the phase transition of the metastable $1T\text{-}MoS_2$ octahedral structure to the $2H\text{-}MoS_2$ trigonal prismatic structure.[8]

An endotherm is observed for $Li_{0.1}MoS_2$ – EDA product and $Li_{0.1}MoS_2(H_2O)_x(EtOH)_y$ at approximately 113 °C, reinforcing the finding that EDA did not intercalate. $Li_{0.1}MoS_2(DEO)_{0.10}$ has an endothermic phase transition at 160.3 °C, possibly due to the 2H-MoS_2 to 1T-MoS_2 phase transition. $Li_{0.1}MoS_2(MA)_{0.14}$ has an endothermic phase transition at 95.9 °C presumably due to a phase transition other than the 1T-MoS_2 to the 2H-MoS_2 because it is so low.

Elemental Analysis. Experimental and calculated results are shown in table 7. Elemental analysis was performed to confirm the concentration of the organic intercalated in MoS_2; however, contamination clouded the results. Therefore, the results are not used in accessing the concentration of organic intercalates. Calculated values are based on the concentration of the guest organic as determined by TGA data excluding the mass loss attributed to water and ethanol.

Table 6. Summary of Results from Elemental Analysis.

Intercalate	Calculated %			Experimental %		
	Carbon	Hydrogen	Nitrogen	Carbon	Hydrogen	Nitrogen
$Li_{0.1}MoS_2$. EDA product	0.41	0.59	0.27	3.38	1.34	0.16
$Li_{0.1}MoS_2(DEO)_{0.10}$	3.7	0.51		6.13	0.66	
$Li_{0.1}MoS_2(MA)_{0.14}$	5.57	0.62		11.95	1.63	
$Li_{0.1}MoS_2(H_2O)_x(EtOH)_y$	0.00	1.18		2.81	1.10	

Discussion

Two new compounds, $Li_{0.1}MoS_2(DEO)_{0.10}$ and $Li_{0.1}MoS_2(MA)_{0.14}$, were prepared by the exfoliation – reflocculation process. In contrast, EDA did not form an intercalated compound. The structures of $Li_{0.1}MoS_2(DEO)_{0.10}$ and $Li_{0.1}MoS_2(MA)_{0.14}$ are closely related to $LiMoS_2$ with the 1T-MoS_2 lattice structure. Based on XRD analysis, the compounds are trigonal with P3 crystal symmetry where $a = b = 3.36$ Å and c, which

varies with the intercalate, is 10.20 Å and 9.97 Å for $Li_{0.1}MoS_2(DEO)_{0.10}$ and

$Li_{0.1}MoS_2(MA)_{0.14}$, respectively. The thickness of the intercalated organic layer is

determined by the unit cell expansion, which is the difference in the c lattice parameter of

the intercalated compound and pristine MoS_2. The packing geometry of the organic

compound between the MoS_2 layers depends on the intercalated compound and in each

case only a monolayer is intercalated into the interlayer space.

As a first approximation, the increase in interlayer space should account for the

intercalation of the DEO and MA molecules parallel to the MoS_2 layers. However, the

crystal lattice expansion is 4.05 Å for $Li_{0.1}MoS_2(DEO)_{0.10}$ and 3.82 Å for

$Li_{0.1}MoS_2(MA)_{0.14}$ while the thickness of the DEO and MA molecules (in the lowest

energy conformations[39]) are ~ 4.18 Å and ~ 5.85 Å, respectively. Therefore a change in

the interlayer space is required to intercalate the molecules. Reports have shown that the

host structure can experience a reduction of the coulombic repulsion forces in the

interlayer space, for layered compounds such as MoS_2, due to alleviation of charge –

charge interactions when intercalated.[17] Therefore intercalates can interdigitate within

the host framework allowing intercalation into a smaller interlayer space.[31] The

calculated thickness of the DEO molecules is ~ 0.13 Å greater than the increase in

interlayer space for $Li_{0.1}MoS_2(DEO)_{0.10}$. Therefore, it is reasonable to think that the DEO

molecules interdigitate with the sulfur layers in MoS_2 to intercalate. Figure 16 shows the

structural model of $Li_{0.1}MoS_2(DEO)_{0.10}$.
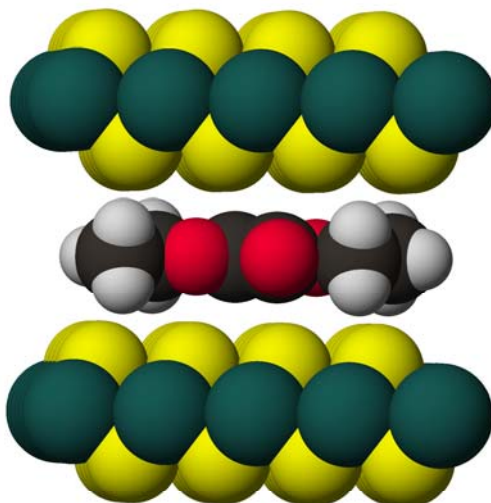
Figure 16. Space filling model of the intercalated compound $Li_{0.1}MoS_2(DEO)_{0.10}$, drawn to scale. The color scheme is as follows: molybdenum, green; sulfur, yellow; carbon, black; hydrogen, gray; oxygen, red.

The structure of the MA molecules must significantly change to account for the ~ 2 Å difference between the MA intercalate thickness and the increase in interlayer space. The lowest energy conformation of MA (see figure 17) has a thickness of ~ 5.85 Å, however if the MA molecule accepts a twist-boat configuration it will have a thickness of ~ 4.32 Å.
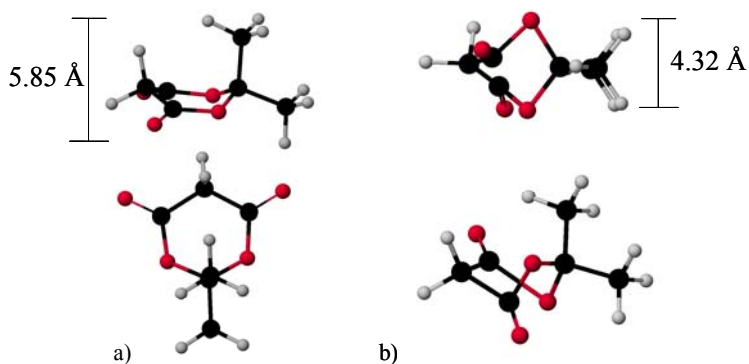
Figure 17. Ball-and stick drawing of a) the lowest energy conformation of Meldrum's Acid and b) the twist-boat conformation of MA.

Like $Li_{0.1}MoS_2(DEO)_{0.10}$, the twist-boat conformation of MA should interdigitate with the sulfur layers in MoS_2 thus allowing the MA molecules to intercalate into the interlayer space of MoS_2, as seen in figure 18.

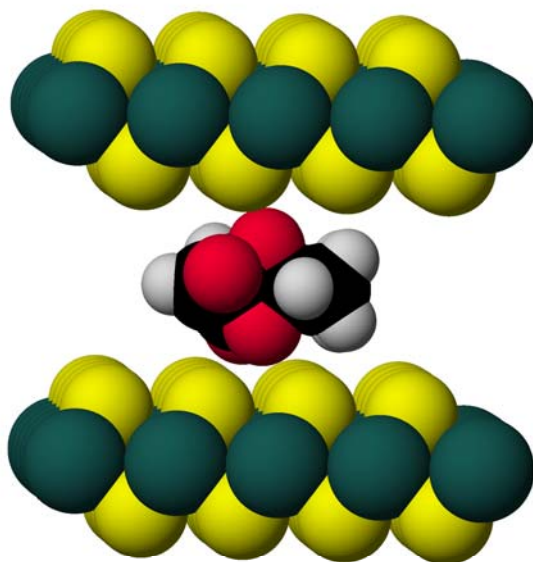
Figure 18. Space filling model of the intercalated compound $Li_{0.1}MoS_2(MA)_{0.14}$, drawn to scale. The color scheme is as follows: molybdenum, green; sulfur, yellow; carbon, black; hydrogen, gray; oxygen, red.

Comparison of the experimental molar ratios with the maximum allowable molar ratios assuming dense packing suggests that DEO and MA molecules form monolayers. For example, densely packed DEO molecules oriented parallel to the MoS_2 layers have an area of ~ 45 $Å^2$ / molecule. The layer area of MoS_2 attributed to each molybdenum atom is 8.6 $Å^2$.[40] The ratio of the two areas determines a maximum concentration of organic that can be intercalated of 0.16 mole of DEO per mole of molybdenum, which is in good agreement with the experimental concentration calculated using air TGA data (0.10). Similarly, densely packed planar MA molecules oriented parallel to the MoS_2 layers have an area of ~ 60 $Å^2$ / molecule. This area translates into a maximum number of intercalated MA molecules per moles of molybdenum of 0.14 mole which is in

excellent agreement with the experimental molar ratio calculated using air TGA data for MA (0.14).

TGA curves were used to understand the thermal decomposition of the organic material within the host framework and to quantify the concentration of organic in the intercalated compound. In air and nitrogen experiments, $Li_{0.1}MoS_2(DEO)_{0.10}$ and $Li_{0.1}MoS_2(MA)_{0.14}$ experience similar weight losses, respectively, in the reformation of MoS_2, as observed by XRD analysis. At approximately 130 °C a sharp mass loss is observed for $Li_{0.1}MoS_2(DEO)_{0.10}$ in both air and nitrogen and is attributed to the decomposition of the intercalated compound by sublimation of the DEO intercalate. In air and nitrogen a continuous mass loss from approximately 122 °C to 300 °C is observed, for $Li_{0.1}MoS_2(MA)_{0.14}$ which is attributed to the deintercalation of the MA intercalate from the intercalated compound. The continuous mass loss is presumably due to the stability in $Li_{0.1}MoS_2(MA)_{0.14}$. The thermal behavior of the intercalated compounds indicates that the intercalated DEO and MA molecules diffuse out of the compound intact rather than decompose within the MoS_2 layers.

At 600 °C both intercalated compounds decomposed to MoS_2 and trace amounts of Li_2MoO_4 in a nitrogen environment, as shown by XRD analysis. The formation of Li_2MoO_4 is not seen in pure MoS_2 and is attributed to the presence of lithium and oxygen in the intercalated compounds. The mixture of products presents a challenge when accurately determining the stoichiometric amount of intercalate in the synthesized intercalated compounds.

The molar ratio of organic present in the final product was determined based on the complete thermal decomposition of $Li_{0.1}MoS_2(DEO)_{0.10}$ and $Li_{0.1}MoS_2(MA)_{0.14}$ to MoO_3 in air. The overall decomposition for MoS_2 in air is seen in equation 6.

$$2MoS_2 + 7O_2 \rightarrow 2MoO_3 + 4SO_2 \qquad\qquad (6)$$

The exact mechanism for decomposition is unknown but it is reasonable to conclude that reaction may proceed through MoS_2O and MoS_2O_2 intermediates.[41]

It has been well documented that the intercalation process is reversible upon heating or aging.[42] After approximately one month or heating to approximately 250 °C, the DEO will diffuse out of the $Li_{0.1}MoS_2(DEO)_{0.10}$ resulting in the thermodynamically stable 2H-MoS_2 polymorph. Similarly, $Li_{0.1}MoS_2(MA)_{0.14}$ will revert to the 2H structure when heated to approximately 300 °C, however, aging for six months does not result in significant decomposition. Presumably, the intercalated DEO and MA stabilize the 1T-MoS_2 structure due to the dipolar interactions with the sulfur layers, therefore the structural transition to the thermodynamically stable 2H polymorph occurs at a higher temperature than the unintercalated 1T-MoS_2. The restacked 2H-MoS_2 will not be as crystalline as pristine 2H-MoS_2 due to lattice imperfections as evidenced by the broad peaks observed in XRD analysis.

Attempts to disperse MoS_2 particles for use as a smoke and obscurant by intensely heating the intercalated system were unsuccessful due too rapid intercalate diffusion at low temperatures.

Conclusion

We have successfully intercalated diethyl oxalate and Meldrum's acid into MoS_2 using a modified exfoliation – reflocculation process described in the literature.[35] Ethyl

diazoacetate did not form an intercalated compound under identical conditions. Formation of $Li_{0.1}MoS_2(DEO)_{0.10}$ and $Li_{0.1}MoS_2(MA)_{0.14}$ was shown by theoretical modeling of molecular packing, air and nitrogen TGA, and ^1H NMR within a standard deviation.

The intercalation with DEO and MA was presumably successful due to the molecular interactions between organic molecule and the sulfur layers. It is reasonable to think that intercalation with EDA, which can be characterized as a zwitterions (see figure 4), was unsuccessful due to the dual charge on the molecule. The charge – charge interaction between the sulfur layer and the nitrogen did not allow the intercalation of EDA suggesting that the ethanolic solvent was able to preferentially intercalate into the MoS_2 layers.

When heated, the intercalated compounds decompose by sublimation of the organic intercalate and therefore do not generate the gas molecules necessary for MoS_2 particle dispersion making it a poor smoke and obscurant technology. Therefore, future smokes and obscurants studies should focus on two methods: (1) intercalation of metallic compounds that retain their metallic nature upon intercalation or deintercalation and (2) functionalizing the surface of metallic structures with highly explosive materials like TNT or RDX. The decomposition of the explosive compounds, within the crystal lattice or on the surface of a metallic compound, may be able to achieve metallic particle dispersion for use as a smoke and obscurant. Examples of layered metallic structures that are capable of being functionalized or intercalated in processes similar to the one described in this study include $NbSe_2$, VSe_2, or other group V dichalcogenides.[43] Upon detonation of the explosives, the intercalated or functionalized metallic structure should

completely disperse. These innovative approaches for new smokes and obscurants

technologies will provide effective real time military asset protection.

(1)	Benavente, E.; Santa Ana, M. A.; Mendizabal, F.; Gonzalez, G. *Coord. Chem. Rev.* **2002**, *224*, 87-109.

(2)	Petkov, V.; Billinge, S. J. L.; Larson, P.; Mahanti, S. D.; Vogt, T.; Rangan, K. K.; Kanatzidis, M. G. *Phys. Rev. B* **2002**, *65*.

(3)	Subba Rao, G. S., M. W. In *Intercalated Layered Materials*; Levy, F., Ed.; Reidel Publishing Company: Holland, 1979; Vol. 6, pp 99-199.

(4)	Brec, R.; Deniard, P.; Rouxel, J. In *Progress in Intercalation Research*; Schollhorn, R., Ed.; Kluwer Academic Publishers: Netherlands, 1994; Vol. 17, pp 177-221.

(5)	Py, M. A.; Haering, R. R. *Can. J. Phys.* **1983**, *61*, 76-84.

(6)	Rao, C. N. R.; Gopalakrishnan, J. *New Directions in Solid State Chemistry*; 2nd ed.; Cambridge Univeristy Press: United Kingdom, 1997.

(7)	Lemmon, J. P.; Wu, J. H.; Oriakhi, C.; Lerner, M. M. *Electrochim. Acta* **1995**, *40*, 2245-2249.

(8)	Kanatzidis, M. G.; Bissessur, R.; Degroot, D. C.; Schindler, J. L.; Kannewurf, C. R. *Chem. Mater.* **1993**, *5*, 595-596.

(9)	O'Hare, D. In *Inorganic Materials*; 2nd ed.; O'Hare, D., Ed.; John Wiley & Sons Ltd: England, 1996, pp 171-254.

(10)	Julien, C.; Saikh, S. I.; Nazri, G. A. *Mater. Sci. Eng., B* **1992**, *15*, 73-77.

(11)	Gonzalez, G.; Santa Ana, M. A.; Sanchez, V.; Benavente, E. *Mol. Cryst. and Liq. Cryst.* **2000**, *353*, 301-308.

(12)	Disalvo, F. J.; Hull, G. W.; Schwartz, L. H.; Voorhoev.Jm; Waszczak, J. V. *J. Chem. Phys.* **1973**, *59*, 1922-1929.

(13)	Yoffe, A. D. *Solid State Ionics* **1990**, *39*, 1-7.

(14)	Schollhorn, R. In *Inclusion Compounds*; NacNicol, D., Ed.; Academic Press: London, 1984; Vol. 1, pp 249-349.

(15)	Tagaya, H.; Hashimoto, T.; Karasu, M.; Izumi, T.; Chiba, K. *Chem. Lett.* **1991**, 2113-2116.

(16)	Jacobson, A. In *Intercalation Chemistry*; Jacobson, A., Ed.; Academic Press: New York, 1982, pp 229-283.

(17)	Liang, W. Y. In *Intercalation in Layered Materials*; Dresselhaus, M. S., Ed.; Plenum Press: New York, 1986; Vol. 148, pp 31-73.

(18)	Wong, H.-V.; Millett, R.; Evans, J.; Barlow, S.; O'Hare, D. *Chem. Mater.* **1995**, *7*, 210-214.

(19)	Gamble, F. R.; Osiecki, J. H.; Cais, M.; Pisharod. R *Science* **1971**, *174*, 493-497.

(20)	Dines, M. B. *Mat. Res. Bull.* **1975**, *10*, 287-291.

(21)	Mulhern, P. J. *Can. J. Phys.* **1989**, *67*, 1049-1052.

(22)	Chrissafis, K.; Zamani, M.; Kambas, K.; Stoemenos, J.; Economou, N. A.; Samaras, I.; Julien, C. *Mater. Sci. Eng., B* **1989**, *3*, 145-151.

(23)	Kertesz, M.; Hoffmann, R. *J. Am. Chem. Soc.* **1984**, *106*, 3453-3460.

(24)	Woollam, J. A.; Somoano, R. B. *Mater. Sci. Eng.* **1977**, *31*, 289-295.

(25)	Yang, D.; Sandoval, S. J.; Divigalpitiya, W. M. R.; Irwin, J. C.; Frindt, R. F. *Phys. Rev. B* **1991**, *43*, 12053-12056.

(26)   Zhou, X.; Yang, D.; Frindt, R. F. *J. Phys. Chem. Solids* **1996**, *57*, 1137-1140.

(27)   Lemmon, J. P.; Lerner, M. M. *Chem. Mater.* **1994**, *6*, 207-210.

(28)   Sanchez, V.; Benavente, E.; Ana, M. A. S.; Gonzalez, G. *Chem. Mater.* **1999**, *11*, 2296-2298.

(29)   Golub, A. S.; Shumilova, I. B.; Novikov, Y. N.; Mansot, J. L.; Danot, M. *Solid State Ionics* **1996**, *91*, 307-314.

(30)   Golub, A. S.; Shumilova, I. B.; Zubavichus, Y. V.; Jahncke, M.; SussFink, G.; Danot, M.; Novikov, Y. N. *J. Mater. Chem.* **1997**, *7*, 163-167.

(31)   Benavente, E.; Sanchez, V.; Ana, M. A. S.; Gonzalez, G. *Mol. Cryst. and Liq. Cryst.* **2000**, *354*, 457-462.

(32)   Bissessur, R.; Haines, R. I.; Bruning, R. *J. Mater. Chem* **2003**, *13*, 44-49.

(33)   Kosidowski, L.; Powell, A. V. *Chem. Commun.* **1998**, 2201-2202.

(34)   Jade 5.0 ed.; Materials Data Inc: Livermore, CA, 1999.

(35)   Powell, A. V.; Kosidowski, L.; McDowall, A. *Mol. Cryst. and Liq. Cryst.* **2000**, *341*, 929-934.

(36)   Joensen, P.; Frindt, R. F.; Morrison, S. R. *Mat. Res. Bull.* **1986**, *21*, 457-461.

(37)   Oriakhi, C. O.; Nafshun, R. L.; Lerner, M. M. *Mat. Res. Bull.* **1996**, *31*, 1513-1520.

(38)   Kanzaki, Y.; Watanabe, N.; K, M.; Matsumoto, O. *J. Phys. Chem.* **1987**, *91*, 2727-2729.

(39)   CAChe 4.1.1 ed.; Oxford Molecular Ltd., 1999.

(40)   Golub, A. S.; Zubavichus, Y. V.; Slovokhotov, Y. L.; Novikov, Y. N.; Danot, M. *Solid State Ionics* **2000**, *128*, 151-160.

(41)   Wei, X.; Zeng, H. *Chem. Mater.* **2003**, *15*, 433-442.

(42)   Bissessur, R.; Schindler, J. L.; Kannewurf, C. R.; Kanatzidis, M. *Mol. Cryst. Liq. Cryst. Sci. Technol., Sect. A* **1994**, *244*, A249-A254.

(43)   Bayard, M.; Mentzen, B.; Sienko, M. *Inorg. Chem.* **1976**, *15*, 1763-1767.